

Surface electronic states of the partially hydrogenated diamond C(100)-(2×1):H surface

Kirill Bobrov, Geneviève Comtet, Gérard Dujardin, and Lucette Hellner

*Laboratoire pour l'Utilisation du Rayonnement Electromagnétique (LURE), Bâtiment 209D, Université Paris-Sud,
91405 Orsay Cedex, France*

and Laboratoire de Photophysique Moléculaire, Bâtiment 210, Université Paris-Sud, 91405 Orsay Cedex, France

Philippe Bergonzo and Christine Mer

*Commissariat à l'Énergie Atomique (CEA), Département d'Instrumentation et de Métrologie, Centre d'Etudes de Saclay,
F-91191 Gif-sur-Yvette Cedex, France*

(Received 2 October 2000; published 4 April 2001)

Surface electronic states of the partially hydrogenated diamond C(100)-(2×1):H surface were studied by near-edge x-ray absorption fine structure and C 1s core level photoemission. Partially hydrogenated surfaces were prepared by synchrotron irradiation of the monohydride-terminated surface or by hydrogen adsorption on the clean surface. A new surface core-exciton state produced at a photon energy of 282.5 eV has been assigned to single dangling bonds of the partially hydrogenated surface. Monitoring this new feature has been found to be a powerful method to study hydrogen kinetics during (i) photon irradiation of a fully hydrogenated diamond surface, (ii) adsorption of atomic hydrogen on a clean diamond surface, and (iii) photon irradiation of a fully hydrogenated surface followed by thermal annealing. From the analysis of dangling-bond distribution, it follows that no preferential pairing of hydrogen on the C-C dimers occurs during hydrogen adsorption at room temperature. In contrast, thermal annealing induces pairing of the single dangling bonds into the π -bonded configuration, the pairing process being accompanied by hydrogen desorption. This observation suggests that the activation barrier of hydrogen thermal diffusion is only slightly lower than that of thermal desorption.

DOI: 10.1103/PhysRevB.63.165421

PACS number(s): 78.70.Dm, 79.20.La, 79.60.Bm, 73.20.At

I. INTRODUCTION

In recent years the electronic structure of the hydrogenated and clean diamond surfaces has been a topic of large interest. This is motivated by the fact that the properties of diamond surfaces depend strongly on the presence of hydrogen. The hydrogenated diamond surface shows a negative electron affinity (NEA), whereas the clean surface has a positive electron affinity.¹ This makes the hydrogenated diamond surface an excellent candidate for fabrication of high-efficiency photon detectors.² Another property of hydrogen is to passivate the surface towards chemical reactivity. After removing hydrogen atoms at selected areas on the surface, one can take advantage of the enhanced reactivity of the resulting dangling bonds for producing templates. Nanofabrication on such templates has been already successfully performed using selective oxidation, nitridation, and metallization of the patterned Si(100)-(2×1):H surface.³ To precisely control and characterize the formation and the physical and chemical properties of hydrogenated and/or dehydrogenated areas on diamond surfaces, it is essential to know the electronic structure of the various hydrogenated and dehydrogenated surface sites.

All previous studies of the C(100)-(2×1) surface have been limited so far to clean or fully hydrogenated surfaces,^{4–6} and nothing is known about the partially hydrogenated surfaces. In this paper, we investigate the electronic structure of partially hydrogenated C(100)-(2×1) diamond surfaces using near-edge x-ray absorption fine structure (NEXAFS) and C 1s photoemission spectroscopy. Partially hydrogenated diamond surfaces are produced either by photon irradiation using an unmonochromatized synchrotron radiation or by atomic hydrogen exposure of the clean surface. In addition to the surface electronic states previously ob-

served on the clean diamond surface, a new surface core-exciton state has been discovered and assigned to single dangling bonds on the surface. This new ability of using NEXAFS spectroscopy to monitor amounts of single dangling bonds and π -bonded dangling bonds is demonstrated to be a powerful tool for exploring the kinetics of hydrogen surface processes. This is illustrated here by exploring the hydrogen surface processes during photon irradiation of the fully hydrogenated surface, atomic hydrogen adsorption on the clean surface, and thermal annealing of the already photon-irradiated surface.

II. EXPERIMENT

A semiconducting boron-doped (type IIb) natural single-crystal diamond with a polished surface of the (100) direction (size 1×6×0.2 mm) was used in our study. Prior to insertion into a ultrahigh vacuum chamber ($P=4\times 10^{-11}$ Torr) the diamond surface was *ex situ* saturated with hydrogen in a microwave (MW) hydrogen plasma at 800 °C for 1 h. The details on the hydrogenation procedure can be found elsewhere.⁷

The clean diamond surface was prepared *in situ* by resistively heating the hydrogenated C(100)-(2×1):H surface mounted on a molybdenum holder. As the diamond is transparent in the infrared light range, which is commonly used to monitor the temperature with a pyrometer, the following procedure to control the annealing process was used. The NEA peak in secondary-electron emission spectra, which is a characteristic of the hydrogenated surface, was used as an indication of the hydrogen presence on the surface. The diamond was heated at a certain temperature (measured on the molybdenum holder) for 1 min; then it was cooled down and secondary-electron spectra were recorded. In case the surface

still demonstrated negative electron affinity, the annealing was repeated at 20–30 °C higher temperature. The procedure was stopped when the NEA peak completely disappeared. This procedure, which relies on the hydrogen coverage only, eliminates any risk of overheating and graphitization of the diamond surface.

The activated hydrogen adsorption was done *in situ* on the clean diamond C(100)-(2×1) surface. Hydrogen was introduced into the UHV chamber through a variable leak valve via a liquid-nitrogen trap. The activation of molecular hydrogen at a pressure of 10^{-8} – 10^{-7} Torr for 1 to 10 min depending on the exposure dose was done using a tungsten filament heated at 1800 °C and located at about 1 cm from the sample. The efficiency of the hot filament to dissociate molecular hydrogen is not known. Therefore the adsorption doses were calculated by multiplying the hydrogen pressure (Torr) and the exposure time (sec).

Photoemission C 1s spectra were recorded using the synchrotron radiation source of Super-ACO in Orsay. In order to improve the surface sensitivity the photon energy was chosen to be 318 eV so that the kinetic energy of escaping C 1s photoelectrons was around 35 eV. This kinetic energy corresponds to the minimum of the electron escape depth and provides the highest possible surface sensitivity of the photoemission spectra.⁸ Emitted photoelectrons were analyzed using a hemispherical electrostatic analyzer with a 250 meV resolution. No charging effects were observed at the applied photon fluxes. The background of secondary electrons was subtracted from the C 1s photoemission spectra. This background was recorded at 325 eV photon energy in the same electron kinetic energy range as the C 1s spectra, since at this photon energy the appropriate separation with C 1s photoelectrons could be achieved.

NEXAFS spectra were recorded in the partial electron yield mode by detecting secondary electrons of 35 eV kinetic energy. As in the case of C 1s photoemission, the 35 eV kinetic energy was chosen in order to achieve the highest surface sensitivity. The photon energy was calibrated using the second absolute band gap of diamond at 302.4 eV (Ref. 9).

Both NEXAFS and photoemission spectra were recorded at the photon incident angle of 68° in order to further improve the surface sensitivity. In our experimental setup the angle between the photon beam and the electron analyzer axis was 90°. Thus, the electron emission angle (θ_e) was determined by the preset incident angle and was always 22°. Both C 1s photoemission and NEXAFS spectra were normalized to the photon flux using the drain current from a gold mesh as a monitor of the photon beam intensity.

The irradiation of the diamond surface was carried out *in situ* at room temperature using the synchrotron radiation source. The hydrogenated diamond C(100)-(2×1):H surface was exposed to the unmonochromatized ($h\nu = 150$ – 600 eV) synchrotron radiation (zero order of the monochromator) for up to 2 h. The relative irradiation doses were calculated by multiplying the gold mesh current (μ A) with the irradiation time (min).

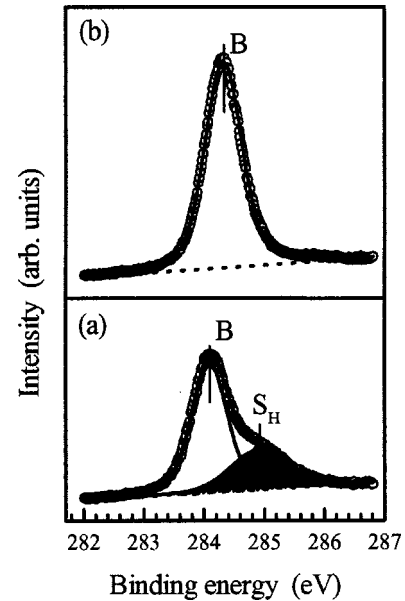


FIG. 1. C 1s photoemission spectra of the hydrogenated diamond C(100)-(2×1):H surface: (a) “as MW-hydrogenated” and (b) the MW-hydrogenated surface after mild annealing. The open circles and dotted lines represent the original C 1s spectra and the background of secondary electrons, respectively. The thin solid lines represent the deconvoluted C 1s components (see Appendix A). The thick solid lines (almost coincident with the original spectra) represent the superposition of the deconvoluted C 1s components. The shadow area represents the S_H component.

III. RESULTS

We used two methods for producing the partially hydrogenated diamond C(100)-(2×1):H surface. In the first method we started from the monohydride-terminated surface. Hydrogen was partially removed from this surface by photon-stimulated desorption using synchrotron radiation as an excitation source. In the second method we started from the clean diamond surface. Atomic hydrogen was then adsorbed *in situ* to produce a submonolayer coverage. In order to study the surface electronic structures and to characterize the dangling-bond distribution on the surface, C 1s photoemission and NEXAFS spectra were recorded.

A. Partially hydrogenated surface prepared by photodesorption

Starting from the fully hydrogenated surface as produced by microwave hydrogenation, we first checked the C 1s structure by photoemission. The “as-prepared” surface shows two components in the C 1s photoemission spectrum [Fig. 1(a)]. The main peak, labeled B, is assigned to the bulk/monohydride C 1s component.¹⁰ The S_H component, located at higher binding energies, is assigned to the CH_x groups on the surface, which are known to be produced by microwave hydrogenation.¹⁰ In order to achieve the pure monohydride termination and to remove the CH_x impurities, mild thermal annealing was done *in situ*. The annealing of the as-prepared diamond surface was repeated several times

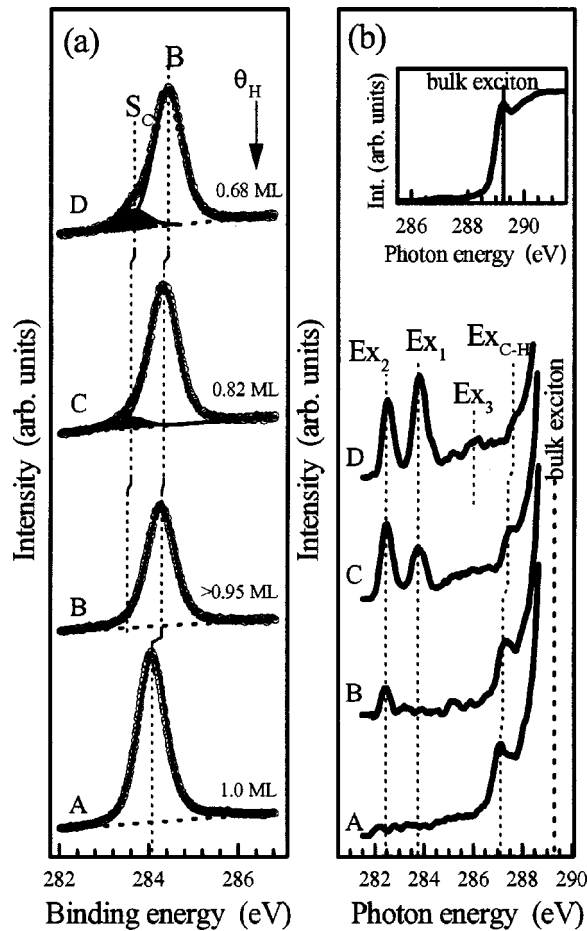


FIG. 2. (a) C 1s photoemission spectra and (b) NEXAFS spectra of the fully hydrogenated diamond C(100)-(2×1):H surface as a function of the synchrotron irradiation dose: curve A, no irradiation was done; curve B, 51 μ A min, curve C, 210 μ A min; and curve D, 344 μ A min. (a) The open circles and dotted lines represent the original C 1s spectra and the background of secondary electrons, respectively. The thin solid lines represent the deconvoluted C 1s components (see Appendix A). The thick solid lines (almost coincident with the original spectrum) represent the superposition of the deconvoluted C 1s components. The shadow areas represent the S_C component (see Sec. IV A). For each irradiation dose the hydrogen coverage (θ_H) was calculated by Eq. (1) as described in Sec. IV A. (b) The diamond bulk exciton is shown in the insert.

at progressively increased temperature until the S_H shoulder in the C 1s photoemission spectra completely disappeared [Fig. 1(b)].

The monohydride-terminated surface, prepared by such a way, was then irradiated with synchrotron radiation at different doses in order to vary the hydrogen coverage on the surface. The corresponding C 1s photoemission and NEXAFS spectra are shown in Fig. 2(a) and 2(b), respectively. The following changes in the C 1s spectra were observed during the irradiation. The bulk component B was slightly shifted to higher binding energies [Fig. 2(a)]. Simultaneously, the shoulder S_C appears in the spectra [Fig. 2(a)].

Considering the NEXAFS spectra, we will concentrate on the *surface* resonances, i.e., the resonances appearing in the band gap below the bulk excitation threshold. The bulk ex-

citon, appearing in all NEXAFS spectra at 289.3 eV photon energy, is shown in the insert of Fig. 2(b). In other NEXAFS spectra only the position of the bulk exciton is indicated. Significant changes induced by the irradiation are observed in the NEXAFS spectra [Fig. 2(b)]. The Ex_{C-H} peak, initially observed on the monohydride-terminated surface, decreased in intensity and gradually transformed into a shoulder [curves B–D in Fig. 2(b)]. A peak, labeled Ex_2 , appears at lowest irradiation dose [curve B in Fig. 2(b)]. At higher doses (curves C and D) the Ex_2 peak continues to increase in intensity, while another peak, labeled as Ex_1 , appears in the spectra and increases in intensity as well.

B. Partially hydrogenated surface prepared by *in situ* hydrogen adsorption

Hydrogen was adsorbed *in situ* on the clean diamond surface at doses in the 2–132 L range (1 L=1 Langmuir = 10^{-6} Torr sec). The corresponding C 1s photoemission and NEXAFS spectra as a function of hydrogen exposure are shown in Figs. 3(a) and 3(b), respectively. The following changes in the C 1s photoemission spectra [Fig. 3(a)] are observed. The bulk component B is slightly shifted to lower binding energies, whereas the S_C shoulder gradually decreases in intensity and finally disappears at high exposure doses. The NEXAFS spectra were changed significantly during the hydrogen adsorption [Fig. 3(b)]. The Ex_{C-H} peak reappears in the spectra. The Ex_1 peak, dominating the spectrum of the clean surface [curve A in Fig. 3(b)], monotonically decreases in intensity and finally disappears at high adsorption doses. More complex behavior is demonstrated by the Ex_2 peak. This peak, which does not exist on the clean surface [curve A in Fig. 3(b)], appears at the lowest adsorption dose (curve B), reaches its maximum at about 8–16 L (curves C and D), and then decreases down to reach a very low intensity at an adsorption dose of 132 L (curve F).

C. Thermal annealing of the partially hydrogenated surface

Finally, we studied the influence of thermal annealing on the dangling-bond distribution of the partially hydrogenated surface. For that purpose, in a separate experiment, the partially hydrogenated surface was prepared by synchrotron irradiation at a certain dose. Then, the partially hydrogenated surface was annealed at progressively increasing temperatures until the clean diamond surface was obtained. The diamond temperature was not measured in this case, although the annealing process was controlled by the method described in Sec. II. After each annealing step the sample was cooled down to room temperature and C 1s and NEXAFS spectra were recorded [Figs. 4(a) and 4(b), respectively]. During the annealing, the bulk component B is shifted to higher binding energies, whereas the S_C shoulder increases in intensity with the annealing [Fig. 4(a)]. The Ex_1 peak intensity in the NEXAFS spectra [Fig. 4(b)] monotonically increases until it reaches the maximum on the clean surface. The Ex_2 peak gradually decreases in intensity and disappears [curve D in Fig. 4(b)] before the clean surface is obtained.

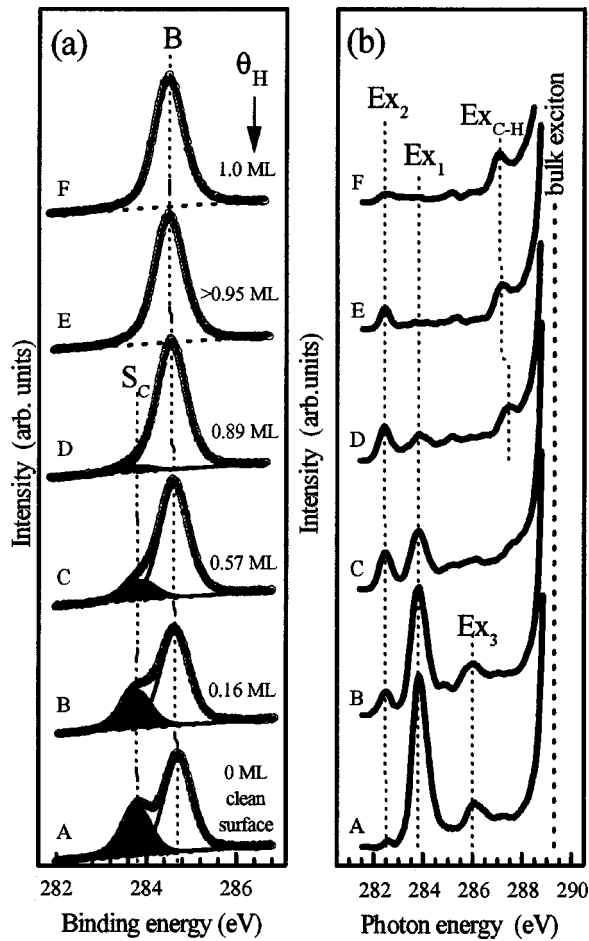


FIG. 3. (a) C 1s photoemission spectra and (b) NEXAFS spectra of the clean diamond C(100)-(2 \times 1) surface as a function of hydrogen exposure: curve A, no adsorption was done; curve B, 2 L; curve C, 8 L; curve D, 16 L; curve E, 32 L; and curve F, 132 L. (a) The same notation for the symbols and curves as in Fig. 2(a) was used. The shadow areas represent the S_C component (see Sec. IV A). For each adsorption dose the hydrogen coverage (θ_H) was calculated by Eq. (1) as described in Sec. IV A.

IV. DISCUSSION

Diamond bulk exciton, located at 289.3 eV photon energy [insert of Fig. 2(b)], was observed in all the NEXAFS spectra of clean, fully hydrogenated, and partially hydrogenated diamond C(100)-(2 \times 1) surfaces. Both the intensity and the position of the bulk exciton were independent of the surface treatment. The bulk exciton is known to be 0.25 eV below the conduction band minimum¹¹ (CBM).

We have observed four surface resonances, Ex_1 , Ex_2 , Ex_3 , and Ex_{C-H} in the NEXAFS spectra of the diamond C(100)-(2 \times 1) surface [Figs. 2(b), 3(b), and 4(b)]. The Ex_1 and Ex_3 resonances, located at 283.8 and 286.0 eV photon energies, respectively, have been previously assigned to the surface core resonances associated with π -bonded dangling bonds of the C-C dimers on the clean diamond C(100)-(2 \times 1) surface.¹¹ The Ex_{C-H} resonance located at 287.1 eV was previously observed on the fully hydrogenated surface for the first time by Hoffman *et al.* and interpreted as an electron transition from C 1s level to the unoccupied σ^* antibonding

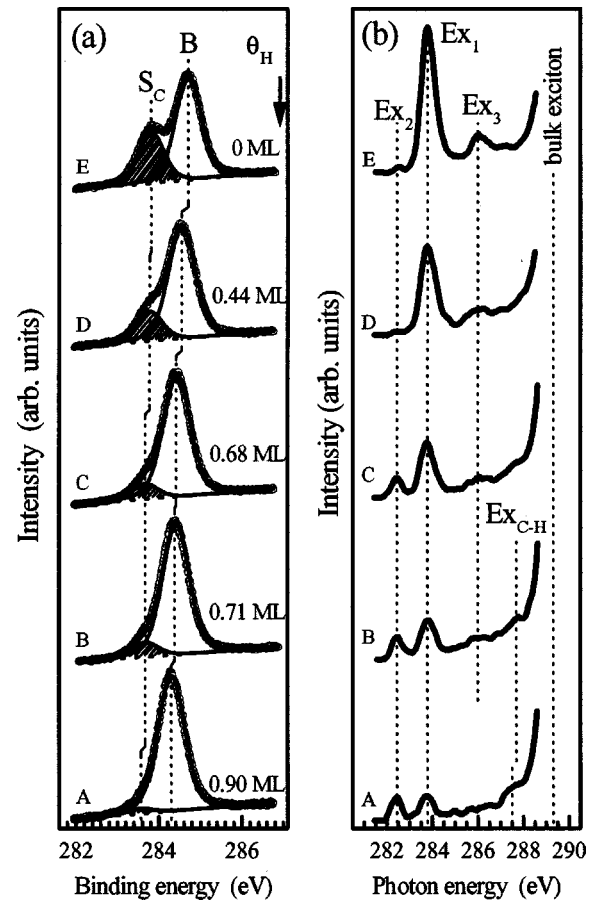


FIG. 4. (a) C 1s photoemission spectra and (b) NEXAFS spectra of the hydrogenated diamond C(100)-(2 \times 1):H surface, synchrotron irradiated at a certain dose, as a function of thermal annealing: curve A, no annealing was done; curves B–E, progressively increased temperature. (a) The same notation for the symbols and curves as in Fig. 2(a) was used. The shadow areas represent the S_C component (see Sec. IV A). For each annealing step the hydrogen coverage (θ_H) was calculated by Eq. (1) as described in Sec. IV A.

state of the C-H monohydride.⁹ This assignment was confirmed later by Graupner *et al.*¹¹

In this paper we report a new resonance Ex_2 , located at a 282.5 eV photon energy, which is characteristic of the diamond C(100)-(2 \times 1) surface with a submonolayer coverage only. In Sec. IV B we will discuss the origin of this Ex_2 resonance and its correlation with the H coverage in terms of single dangling bonds produced on the partially hydrogenated diamond surface. We will demonstrate in Sec. IV C that the Ex_2 resonance provides unique possibility to calculate quantitatively the distribution of dangling bonds between single and π -bonded configurations and to shed light on the kinetics of hydrogenation/dehydrogenation processes on the diamond surface.

A. Characterization of the partially hydrogenated C(100)-(2 \times 1):H surface

To clarify the processes occurring on the diamond surface under hydrogen adsorption, synchrotron irradiation, and ther-

TABLE I. Deconvolution of the C 1s photoemission spectra of the diamond C(100)-(2×1) surfaces.

Surface	C 1s components	Chemical shift (eV)	FWHM ^a (eV)
As MW-hydrogenated	<i>B</i>	+0.8	0.62
	<i>S_H</i>		0.98
Hydrogen adsorbed (fully hydrogenated)	<i>B</i>		0.65
Thermal annealed (clean)	<i>B</i>	−0.9	0.62
	<i>S_C</i>		0.63
Synchrotron irradiated (partially hydrogenated)	<i>B</i>	−0.75	0.64
	<i>S_C</i>		0.61

^aGaussian full width at half maximum.

mal annealing, we will now analyze the corresponding C 1s photoemission spectra [Figs. 2(a), 3(a), and 4(a)]. The photoemission spectra of the partially hydrogenated and clean diamond surfaces were slightly shifted towards higher binding energies compared with the fully hydrogenated surface. This is due to band-bending effects accompanying hydrogen desorption.¹⁰ This phenomenon is, however, beyond of our scope in this study. In this paper we will consider the intensity and the width of the C 1s components only. The C 1s spectra were deconvoluted as described in Appendix A. Two C 1s components only were derived from the actual shape of the photoemission spectra: (i) a bulk component *B*, which coincides with the monohydride component of the C(100)-(2×1):H surface,¹⁰ and (ii) a *S_C*, component which is observed only on the clean surface and has been previously assigned to surface carbon dimers.¹⁰ The *S_H* component, observed previously on the MW-hydrogenated surface¹⁰ and assigned to the CH_x species, is not detected in the C 1s spectra [Figs. 2(a), 3(a), and 4(a)].

We analyzed the width of the bulk component *B* (see Appendix A and Table I) in order to estimate the degree of disordering possibly introduced on the surface by hydrogen adsorption, synchrotron irradiation, and thermal annealing. Indeed, the width of the C 1s line shape has been demonstrated to be very sensitive to the surface defects.¹² In Table I we can see that the *B* component as well as the *S_C* component has essentially the same width for the clean, synchrotron-irradiated, and hydrogen-adsorbed surfaces. It follows that no surface disordering and/or defect formation is expected to exist on the partially hydrogenated diamond surfaces in our case.

Thus, we conclude that the variation of the *S_C* peak intensity in the C 1s photoemission spectra in Figs. 2(a), 3(a), and 4(a) corresponds to the variation of the hydrogen coverage. The hydrogen coverage (θ_H) was calculated using deconvoluted intensities as

$$\theta_H = 1 - S_C(\theta_H)/S_C(\text{clean}), \quad (1)$$

where $S_C(\theta_H)$ is the intensity of the *S_C* component at coverage θ_H and $S_C(\text{clean})$ is the intensity of the *S_C* component for the clean surface.

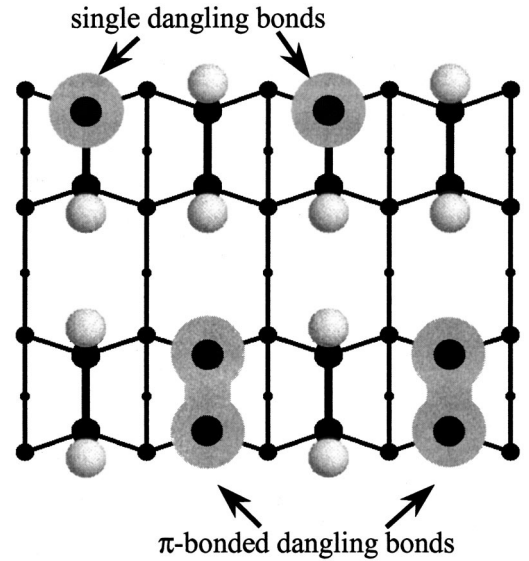


FIG. 5. Schematics of dangling bonds on the hydrogenated diamond C(100)-(2×1):H surface at a submonolayer coverage. The dangling bonds are shown as gray areas whereas the white circles represent hydrogen adatoms. The black circles of different size represent carbon atoms.

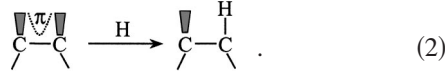
B. Surface resonances as a tool to monitor dangling bonds on the partially hydrogenated surface

We will now explain the behavior of the NEXAFS resonances during synchrotron irradiation [Fig. 2(b)] and hydrogen adsorption [Fig. 3(b)] in terms of hydrogen interaction with dangling bonds. Under hydrogen adsorption, π -bonded dangling bonds of the clean surface are gradually saturated by hydrogen. As a result, the intensities of the Ex_1 and Ex_3 resonances decrease and that of the Ex_{C-H} resonance increases [Fig. 3(b)]. The reverse process occurs during synchrotron irradiation of the hydrogenated surface: light-induced C-H bond breaking creates π -bonded dangling bonds on the surface. Consequently, the intensity of the Ex_1 and Ex_3 resonances increases and the intensity of the Ex_{C-H} resonance decreases [Fig. 2(b)].

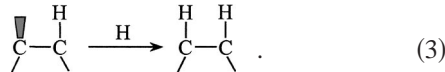
We stress that the behavior of the Ex_2 resonance is more complex. The Ex_2 resonance does not exist on either the fully hydrogenated surface [curve A in Fig. 2(b)] or on the clean surface [curve A in Fig. 3(b)]. It appears only on the surface with a submonolayer hydrogen coverage. We suggest that the Ex_2 resonance originates from the single dangling bonds existing on the diamond surface at a submonolayer hydrogen coverage. In the following we will demonstrate that this suggestion explains the unusual behavior of the Ex_2 resonance intensity during hydrogen adsorption. In Sec. IV C we will show that this is fully consistent with the dangling-bond distribution at submonolayer hydrogen coverage.

The single and π -bonded dangling bonds on the partially hydrogenated surface are shown schematically in Fig. 5. The π -bonded paired dangling bonds are the only type of dangling bonds on the clean surface and, consequently, the Ex_1 and Ex_3 resonances are only present on the clean surface [curve A in Fig. 3(b)]. When a hydrogen atom adsorbs on a clean C-C dimer, it suppresses the electronic coupling be-

tween dangling bonds and produces an uncoupled single dangling bond:

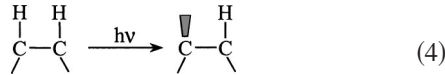


As a result, the Ex_2 resonance appears in the NEXAFS spectrum [curve *B* in Fig. 3(b)]. Further hydrogen adsorption on the clean dimers increases the Ex_2 resonance intensity [curve *C* in Fig. 3(b)]. However, with the increased amount of single dangling bonds another adsorption channel, namely hydrogen adsorption on the single-occupied dimers, becomes important:

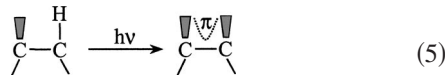


At high H coverage this channel dominates the adsorption. Consequently, the Ex_2 resonance decreases in intensity and finally disappears on the fully hydrogenated surface [curves *D*–*F* in Fig. 3(b)].

The single dangling bonds should also exist on the surface prepared by synchrotron irradiation. Indeed, light irradiation, breaking single C–H bonds in the double occupied dimers, produces single dangling bonds



and the Ex_2 resonance appears in the spectra [Fig. 2(b)]. The second C–H bond breaking of the singly occupied dimers creates a clean π -bonded dimer



accounting for the increased intensity of the Ex_1 and Ex_3 resonances in Fig. 2(b).

Now we will analyze the origin of the electronic transitions giving rise to the Ex_1 , Ex_2 , and Ex_3 surface resonances. As it was demonstrated by Morar *et al.*, the electronic states of the diamond C(111)-(2×1) surface could be classified according their position in the band gap.⁸ The electronic states, lying below the Fermi level, were interpreted as surface core excitons whose energy is influenced by strong electron-hole interaction at the surface.⁸ By contrast, the electronic states above the Fermi level were assigned to unoccupied dangling-bond surface states.⁸

The binding energy of the *B* component of the *in situ* fully hydrogenated surface (284.5 eV) was taken as an actual position of the Fermi level in the band gap. From this the bulk diamond exciton is derived to be 4.8 eV (289.3–284.5 eV) above the Fermi level. The CBM was recently reported to be 0.25 eV above the bulk exciton energy.⁶ The valence-band maximum (VBM) is located 5.47 eV (diamond band gap) below the CBM (Ref. 13). This makes the Fermi level to be located 0.42 eV above the VBM. This is in reasonable agree-

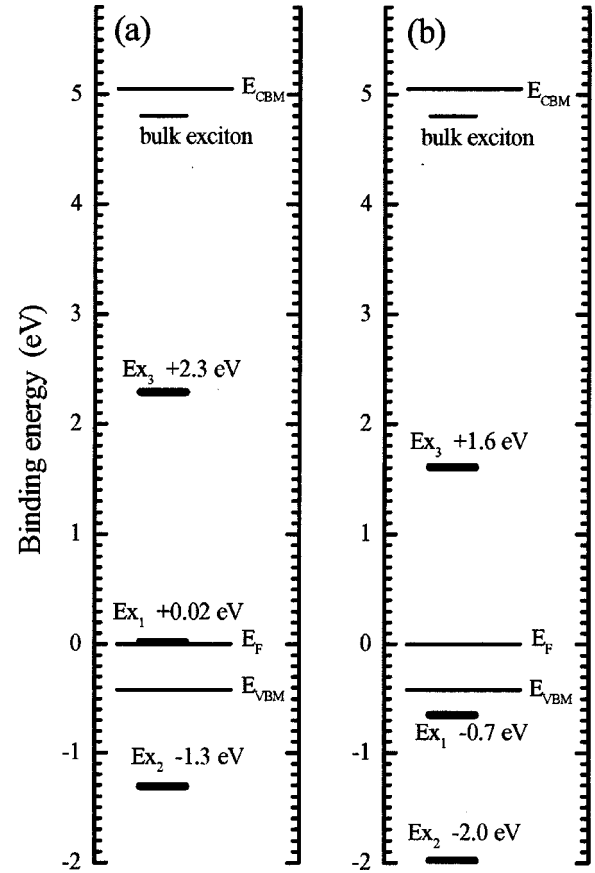


FIG. 6. Schematics illustrating position of the Ex_1 , Ex_2 , and Ex_3 surface resonances with respect to the Fermi level. Binding energies of the resonances were calculated assuming the binding energy of the C 1s hole to be (a) 283.8 eV, which corresponds to the clean surface dimers (S_C component), and (b) 284.5 eV, which corresponds to the bulk diamond (*B* component).

ment with the value of $E_F - E_{\text{VBM}} = 0.3$ eV reported for a highly-boron-doped semiconducting diamond¹ ($N_B = 10^{16} \text{ cm}^{-3}$).

The $\text{Ex}_{\text{C-H}}$, Ex_1 , Ex_2 , and Ex_3 binding energies were calculated from the NEXAFS corresponding resonance energies by assuming an electron-independent model and by considering that the binding energy of the C 1s hole is either that of the clean diamond surface (S_C component at 283.8 eV) or that of the bulk diamond [*B* component at 284.5–284.7 eV (Ref. 14)]. The results are shown in Figs. 6(a) and 6(b), respectively. As mentioned by Graupner *et al.*, one should use the binding energy of the C 1s bulk diamond only if one assumes that the surface shift is mainly due to final-state effects rather than initial-state effects.⁶ In fact, it is very difficult to predict whether final-state effects dominate over initial-state effects in the surface shift of the C 1s binding energy. However, we note that this has an important consequence on the assignment of Ex_1 , Ex_2 , and Ex_3 states.

The Ex_3 resonance always has a positive binding energy independently of which effects—initial state [Fig. 6(a)] or final state [Fig. 6(b)]—dominate on the surface. Thus, the Ex_3 surface resonance most probably corresponds to the electronic excitation into unoccupied π^* -antibonding states

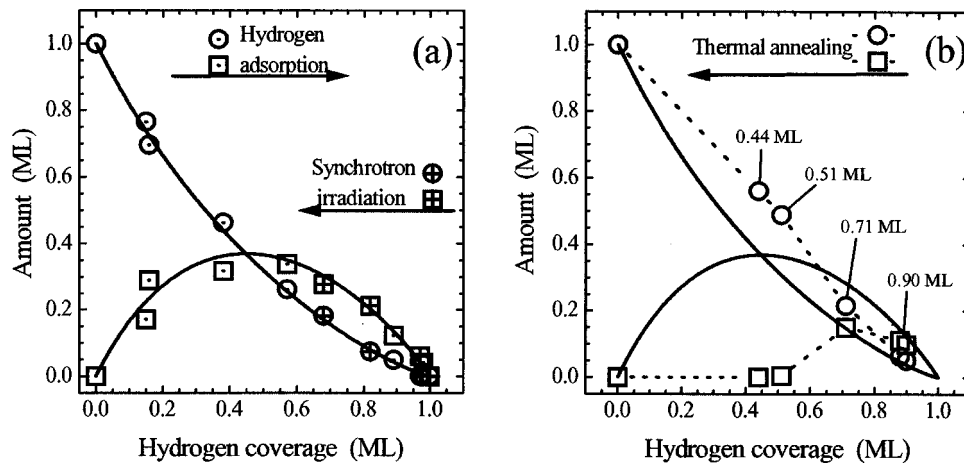


FIG. 7. Dangling-bond distribution on the partially hydrogenated diamond C(100)-(2 \times 1):H surface prepared by (a) hydrogen adsorption on the clean surface and synchrotron irradiation of the fully hydrogenated surface and (b) synchrotron irradiation of the fully hydrogenated surface followed by thermal annealing. The dotted, crossed, and hollow symbols correspond to hydrogen adsorption, synchrotron irradiation, and thermal annealing procedures, respectively. These symbols represent the experimentally deduced values whereas the solid curves represent the numerical solution of kinetic equations (see Appendix B). The squares and circles represent the single and paired (π -bonded) dangling-bond configurations, respectively.

of the clean dimers as was recently suggested by Graupner *et al.*¹¹ The assignment of the Ex_1 resonance is more complicated. In Fig. 6(b), the Ex_1 state is below the Fermi level and should therefore be considered as a core exciton state as discussed by Graupner *et al.*,¹¹ whereas in Fig. 6(a) it is slightly above the Fermi level and could be assigned to an unoccupied surface state like the Ex_{C-H} state. The assignment of the Ex_2 resonance is unambiguous: this resonance represents a core surface exciton since it is always well below the Fermi level whatever the assumption on the binding energy of the C 1s hole.

C. Distribution of dangling bonds on the diamond C(100)-(2 \times 1):H surface with a submonolayer hydrogen coverage

Considering that the Ex_2 core surface exciton is associated with the single dangling bonds, whereas the Ex_1 resonance corresponds to the π -bonded paired dangling bonds, allows us to quantitatively evaluate the dangling-bond distribution between these two configurations. The importance stems from the fact that dangling-bond pairing partially reduces their unsaturated character¹⁵ and, consequently, influences the surface reactivity.

Here we deduce the dangling-bond distribution from the intensities of Ex_1 and Ex_2 resonances in the NEXAFS spectra. Then, the experimentally determined distribution is compared with that obtained by modeling the processes described by Eqs. (2)–(5) (thereafter the random distribution model). Both procedures are described in Appendix B. The dangling-bond distribution of the partially hydrogenated surface was derived in various situations. The first corresponds to the case where no thermal effect is expected on the dangling-bond distribution. It is valid for hydrogen adsorption (Fig. 3) and synchrotron irradiation (Fig. 2). The second situation corresponds to the case in which thermal effects play an essential role. This is valid when the dangling-bond

distribution, initially achieved by synchrotron irradiation, is modified by thermal annealing (Fig. 4). The dangling-bond distributions for these two situations are shown in Fig. 7. The distributions are quite different. It can be seen in Fig. 7(a) that for the nonthermal processes the single dangling bonds exist in the whole range of hydrogen coverage. The amounts of the dangling bonds can be properly described by assuming that after synchrotron irradiation the single dangling bonds, created by hydrogen-atom photodesorption, are randomly distributed over the surface without any pairing effect. Similarly, it is assumed that after atomic hydrogen exposure of the clean surface, the hydrogen atoms are randomly distributed again without any pairing effect. Indeed, in the whole coverage range (θ_H) the experimentally measured amounts of single dangling bonds [circles in Fig. 7(a)] and paired dangling bonds [squares in Fig. 7(a)] correlate well with the theoretically calculated values [solid lines in Fig. 7(a)].

The results shown in Fig. 7(b) demonstrate that the assumption of random distribution and absence of pairing effect is no more valid after thermal annealing. The data in Fig. 7(b) relate to an experiment in which we start with a synchrotron-irradiated surface so that 10% of the surface hydrogen has been photodesorbed [$\theta_H = 0.90$ monolayer (ML)]. At this point both single dangling bonds and π -bonded dangling bonds exist on the surface, and their amounts are described properly by the random distribution model. Then the surface is progressively heated so that the hydrogen coverage decreases to 0.88, 0.71, 0.51, 0.44, and 0 ML (clean surface). It is seen in Fig. 7(b) that the number of single dangling bonds is much smaller (except at 0 ML) than expected from the random distribution model, whereas the number of π -bonded dangling bonds is higher than expected from this model. We conclude that the random distribution model fails in this case.

From the results in Fig. 7(a) and 7(b) the important information on the kinetics of surface-related processes may be

obtained. First, it can be concluded that little or no preferential pairing of hydrogen adatoms on C-C dimers occurs during hydrogen adsorption at room temperature. It means that the rebonding of the dangling bonds (and, consequently, the surface hydrogen adatoms) into the more thermodynamically favorable π -bonded configuration is limited by the very low mobility of hydrogen adatoms. Indeed, the activation barrier for hydrogen hopping on the diamond C(100)-(2 \times 1) surface was calculated to be at least 2.62 eV (Ref. 16). Second, it can be seen that at elevated temperatures (the case of thermal annealing), the thermal-induced redistribution of hydrogen adatoms does occur and results in pairing both hydrogen adatoms and dangling bonds on separate dimers. In that case the π -bonding formation on the clean C-C dimers represents the driving force for pairing. The pairing, however, occurs simultaneously with hydrogen desorption, as can be seen in Fig. 7(b). It implies that the activation energy of the hydrogen diffusion is only slightly lower than the activation energy of hydrogen desorption.

V. SUMMARY AND CONCLUSIONS

Surface electronic states of the partially hydrogenated diamond C(100)-(2 \times 1):H surface have been studied by NEXAFS and C 1s photoemission. The partially hydrogenated surfaces were prepared by (i) synchrotron irradiation of the fully hydrogenated surface and (ii) hydrogen adsorption on the clean diamond surface. A new Ex₂ resonance, in addition to the Ex₁ and Ex₃ resonances of the clean surface, was observed on the partially hydrogenated surface. This resonance is located below the Fermi level and is assigned to single dangling bonds on the surface. Thus, the ability to monitor amounts of both single (Ex₂) and π -bonded (Ex₁) dangling bonds on the surface has been used to study the kinetics of (i) synchrotron irradiation of the fully hydrogenated surface, (ii) atomic hydrogen adsorption on the clean surface, and (iii) thermal annealing of the surface that has already been under synchrotron irradiation. No preferential pairing of hydrogen on the C-C dimers was found during hydrogen adsorption at room temperature. By contrast, thermal annealing induces pairing of the single dangling bonds into the π -bonded configuration. The pairing process is accompanied with hydrogen desorption. We believe that this method of monitoring the relative amounts of single and π -bonded dangling bonds can be very powerful for kinetics studies of a large number of other processes on diamond surfaces.

ACKNOWLEDGMENTS

We wish to thank Professor A. Hoffman for helpful discussion, the AFIRST program, and the European TMR network Surface Photochemistry for financial support.

APPENDIX A

The C 1s photoemission spectra shown in Figs. 1(a), 1(b), 2(a), 3(a), and 4(a) were deconvoluted assuming a mixed Gaussian-Lorentzian line shape (Voigt function) for each C 1s component. The number of C 1s components for each photoemission spectrum was determined from the second de-

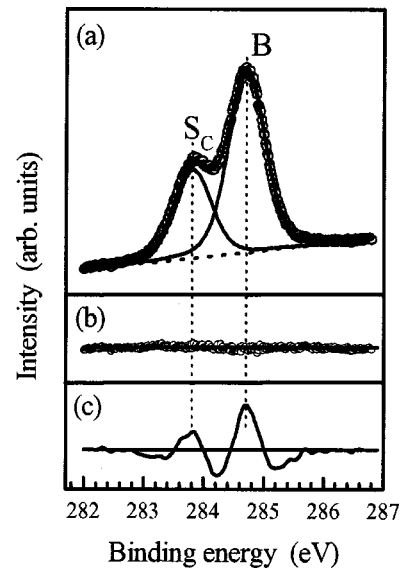


FIG. 8. Deconvolution of the C 1s photoemission spectrum recorded on the clean diamond C(100)-(2 \times 1) surface. (a) Open circles represent the original data, thin solid lines represent the deconvoluted C 1s components, the dotted line shows the background, and the thick solid line represents the superposition of the C 1s components (synthesized spectrum). (b) The open circles represent residual values remaining after subtracting the synthesized spectrum from the original spectrum. (c) Second derivative (negative) of the original photoemission spectrum taken numerically.

rivative spectra ($-d^2N/dE^2$ vs E). An example of the $-d^2N/dE^2$ curve is shown in Fig. 8(c). Three components only, namely, B, S_H, and S_C, were found by the deconvolution analysis. For each C 1s component three parameters—the Gaussian width, binding energy, and intensity—were varied independently and the best-fit criteria was used in the deconvolution. The smallest value of the Lorentz width that allowed us to fit all the C 1s spectra properly was found to be 0.19 eV, and this value was kept fixed throughout the deconvolution.

All the C 1s photoemission spectra were successfully deconvoluted. Deconvolution of the C 1s spectrum of the clean surface is shown in Fig. 8(a). It can be seen that the superposition of the B and S_C components [thick solid line in Fig. 8(a)] properly describes the experimental data [open circles in Fig. 8(a)]. The residual spectrum, taken as the difference between the experimentally measured and synthesized spectra [open circles in Fig. 8(b)], is completely flat and has very low intensity comparable with the noise level. The results of the deconvolution are summarized in Table I. The chemical shifts of the clean surface S_C and hydrocarbon S_H components were found to be -0.9 and $+0.8$ eV, respectively (see Table I). This agrees well with the previously reported values.¹⁰

APPENDIX B

We deduced the dangling-bond distribution on the diamond C(100)-(2 \times 1):H surface using (i) Ex₁ and Ex₂ exciton intensities and (ii) a numerical solution of kinetics equations

for hydrogen adsorption/desorption processes.

(i) The material balance on the diamond surface at a sub-monolayer coverage θ_H may be written as

$$\theta_{\text{NOD}} + \theta_{\text{SOD}} + \theta_{\text{DOD}} = 1, \quad (\text{B1})$$

where θ_{NOD} , θ_{SOD} , and θ_{DOD} are the portions of the surface covered by nonoccupied, singly occupied, and doubly occupied dimers, respectively. The hydrogen coverage is, consequently,

$$\theta_H = \theta_{\text{DOD}} + 0.5\theta_{\text{SOD}}. \quad (\text{B2})$$

Taking into account that each singly occupied dimer contains one carbon associated with the single dangling bond, whereas each nonoccupied dimer contains two carbons associated with the paired dangling bonds, we can write

$$Ex_1 = 2k\theta_{\text{NOD}},$$

$$Ex_2 = k\theta_{\text{SOD}}, \quad (\text{B3})$$

where Ex_1 and Ex_2 are the intensities of the corresponding excitons and k is a coefficient.

Solving Eqs. (B1)–(B3) together we obtain

$$\theta_{\text{paired}}^{\text{DB}} = \theta_{\text{NOD}} = (1 - \theta_H)Ex_1 / (Ex_1 + Ex_2),$$

$$\theta_{\text{single}}^{\text{DB}} = \theta_{\text{SOD}} = 2(1 - \theta_H)Ex_2 / (Ex_1 + Ex_2), \quad (\text{B4})$$

where $\theta_{\text{paired}}^{\text{DB}}$ and $\theta_{\text{single}}^{\text{DB}}$ are the amounts of paired and single dangling bonds, respectively. These amounts are plotted as circles ($\theta_{\text{paired}}^{\text{DB}}$) and squares ($\theta_{\text{single}}^{\text{DB}}$) in Fig. 7.

(ii) The numerical solution of kinetics equations (2)–(5) was done as follows. The reaction rates were assumed to be proportional to the amounts of corresponding dimers at any particular hydrogen coverage. Hydrogen adsorption on the clean surface was assumed to occur on both clean and singly occupied dimers independently. The same adsorption probability of hydrogen was assumed for both clean and singly occupied dimers. Similarly, the same cross section for photon-stimulated desorption was assumed for doubly and singly occupied dimers. In both cases of hydrogen adsorption and light-induced desorption, no hydrogen diffusion was assumed to occur on the diamond surface. The results are shown in Fig. 7 as solid lines.

¹L. Diederich, O. M. Kuttel, P. Aebi, and L. Schlapbach, *Surf. Sci.* **418**, 219 (1998).

²A. Laikhtman, A. Hoffman, R. Kalish, Y. Avigal, A. Breskin, R. Chechik, E. Shefer, Y. Lifshitz, *Appl. Phys. Lett.* **73**, 1433 (1998).

³J. W. Lyding, *Proc. IEEE* **85**, 589 (1997).

⁴L. Diederich, P. Aebi, O. M. Kuttel, E. Maillard-Schaller, R. Fasel, and L. Schlapbach, *Surf. Sci.* **393**, L77 (1997).

⁵R. Graupner, M. Hollering, A. Ziegler, J. Ristein, and L. Ley, *Phys. Rev. B* **55**, 10 841 (1997).

⁶J. Wu, R. Gao, X. Yang, P. Planetta, and I. Lindau, *J. Vac. Sci. Technol. A* **11**, 1048 (1993).

⁷K. Bobrov, H. Shechter, M. Folman, and A. Hoffman, *Diamond Relat. Mater.* **7**, 170 (1998).

⁸J. F. Morar, F. J. Himpsel, G. Hollinger, J. L. Jordon, G. Hughes, and F. R. McFeely, *Phys. Rev. B* **33**, 1346 (1986).

⁹A. Hoffman, G. Comtet, L. Hellner, G. Dujardin, and M. Petravic,

Appl. Phys. Lett. **73**, 1152 (1998).

¹⁰R. Graupner, F. Maier, J. Ristein, L. Ley, and Ch. Jung, *Phys. Rev. B* **57**, 12 397 (1998).

¹¹R. Graupner, J. Ristein, L. Ley and Ch. Jung, *Phys. Rev. B* **60**, 17 023 (1999).

¹²A. Laikhtman, I. Gouzman, A. Hoffman, G. Comtet, L. Hellner, and G. Dujardin, *J. Appl. Phys.* **86**, 4192 (1999).

¹³C. D. Clark, P. J. Dean, and P. V. Harris, *Proc. R. Soc. London, Ser. A* **227**, 312 (1964).

¹⁴The actual value of the binding energy of the *B* component varies from 284.7 eV (clean surface) to 284.5 eV (hydrogenated surface) as a function of hydrogen coverage due to band-bending effects.

¹⁵T. I. Hukka, T. A. Pakkanen, and M. P. D'Evelyn, *J. Phys. Chem.* **98**, 12 420 (1994).

¹⁶E. J. Dawnkaski, D. Srivastava, and B. J. Garrison, *J. Chem. Phys.* **102**, 9401 (1995).